Spectroscopy of Some Artificially Radioactive Nuclei

ALLAN C. G. MITCHELL
Indiana University, Bloomington, Indiana

I. INTRODUCTION

THE subject of nuclear spectroscopy has now advanced to such a stage and the results which have been obtained are numerous enough so that it warrants, at this time, a status report setting forth the findings obtained to date. For convenience, one distinguishes two separate branches of nuclear spectroscopy: That branch in which the energy of essentially "instantaneous" gamma-rays, occurring as a result of the bombardment by high energy particles, is measured; and secondly, that branch in which the energies of gamma-rays and beta-rays of radioactive nuclei are measured. The emission of "instantaneous" gamma-rays is naturally connected with the emission of heavy particles in a nuclear reaction. A review of this field has been given by Hornyak and Lauritsen (H1) and brought up to date by Lauritsen (L1). The results of the work on measurements of radioactive nuclei will be discussed in this report.

The present report is limited to a discussion of the radiations from the artificially radioactive nuclei, no attempt being made to consider the heavy, naturally radioactive nuclei. In addition, the main interest will be in the energy levels of the product nuclei formed as a result of the radioactive decay of the parent. Since pure electron or positron emitters, unaccompanied by gamma-radiation, do not give rise to excited states of the product, they are, of course, omitted. According to the table of Seaborg and Perlman (S1), there are somewhere between 300 and 500 radioactive isotopes known, some of which are pure electron or positron emitters. Of the remainder, about 125 have been investigated to some extent by spectroscopic means. For many of these the spectroscopic work is only fragmentary and no disintegration schemes have been completed. To date, energy level schemes for about 50 nuclei have been worked out in a reasonably satisfactory manner and it is with these that this report will be concerned. In addition, many isomeric and metastable states are known. These have been adequately discussed by Segrè and Helmholz (S2) and will not be considered here except insofar as they contribute to a discussion of the disintegration schemes at hand.

The similarities and differences between the problem of the nuclear spectroscopist in determining nuclear energy levels and that of the atomic spectroscopist in determining atomic energy levels are rather obvious, but it may be worth while to point out a few of them here. In general, the nuclear spectroscopist does not measure the wave-length, frequency, or energy of a nuclear gamma-ray directly, but has to rely on secondary effects, *viz.*, the measurement of the energy of photo-electrons and Compton-electrons ejected from a radiator by the gamma-rays or from internal conversion electrons. From a measurement of the secondary electrons the energy of the gamma-ray may be inferred. The present exception is the use of a curved crystal spectrograph by DuMond (D1, D2) and his group to measure the wave-length of gamma-rays. After the energies of the several gamma-rays have been determined, the problem of constructing the energy level diagram is essentially the same as that in atomic spectroscopy. In most cases, however, the nuclear physicist is able to measure the beta-rays given out by the radioactive parent and can thereby obtain additional checks on the energy levels.

The accuracy obtainable by conventional nuclear spectroscopic methods allows the energy of a given line to be determined to 0.5–2.0 percent, while the separation of two lines differing in energy by about five percent may be accomplished under favorable circumstances. This does not, of course, compare to the resolving power obtainable in atomic spectroscopy. Impurities show up in atomic spectra as weak lines, for the most part, whereas in nuclear spectroscopy, owing to the wide variation in the cross sections for production of radioactive species, a small impurity may show up as an extremely strong line. However, such impurities may be detected by measuring the radioactive decay period associated with all lines.

Finally, in the present state of our knowledge, there appears to be no fine structure associated with gamma-ray levels. This may come about on account of the lack of resolving power of present-day apparatus or, what is probably more likely, it may be caused by the fact that the nucleus is complicated and must be treated as a many-body problem. In any event, there are not as yet any interval and intensity rules in nuclear spectroscopy.

II. APPARATUS AND METHOD

The apparatus employed is usually some device which will focus electrons according to their energy—usually a 180°-type beta-ray spectrograph or a magnetic lens. Many variations of both types of instruments have been described in the literature and need not be discussed here. In general, a Geiger-Müller counter is used to record focused electrons for a given value of the magnetic rigidity ($H\rho$). In some instances, in 180°-type instruments, a photographic plate or film is used to record photo-electron or internal conversion lines.

For the measurement of gamma-rays, the radioactive source is enclosed in a capsule thick enough to stop all disintegration electrons. A thin radiator, usually of lead but sometimes of other materials, is placed over the source and the photo-electrons ejected therefrom by the gamma-rays are measured. The energy of the gamma-ray is related to the energy of the observed electron line by the relation

$$E_\gamma = E_{el} - K$$
$$E_\gamma = E_{el}' - L \text{ etc.}, \quad (1)$$

where K and L denote the value of the K and L absorption edges of the radiator. The relative intensity of the gamma-rays is determined from the relative intensity of their associated K-photo-electrons by the empirical relation given by Gray (G1).

In investigating a given source it is necessary also to measure the momentum distribution of the beta-rays from a thin source. In some cases internal conversion lines will appear superimposed on the continuous electron distribution. In this case the energy of the gamma-ray responsible for the conversion electron may be determined from relations similar to (1), except that K and L are now taken as the absorption edges of the product nucleus. A Fermi plot is then made of the momentum distribution of the disintegration electrons. In many cases this distribution will be found to be complex, consisting of several groups whose end-point energies and relative intensities may be determined. With the help of these end-point energies, and the energies of the gamma-rays, a self-consistent energy level scheme can be constructed.

In order to get a confirmation of the energy level scheme, derived as a result of measurements on the gamma-ray and disintegration electron spectra, it is wise to perform coincidence counting experiments (M1). Sometimes it is possible to do coincidence experiments in the spectrograph and measure the number of coincidences between gamma-rays and resolved beta-rays. In this way a direct check on the disintegration scheme may be obtained. Such experiments are quite tedious and difficult to perform. In many cases, it is sufficient to carry out coincidence experiments in which the energies of the beta-rays are measured by absorption. In either case, when the disintegration scheme is not too complicated, a good confirmation can be obtained.

One of the most important pieces of information which it is desirable to obtain is the value of the total angular momentum associated with each level of the disintegration scheme. Up to the present no great progress has been made in this important phase of the work. There exist possibilities for determining the *change in angular momentum* and parity associated with the emission of a given gamma-ray, a sequence of two gamma-rays, or the emission of a given beta-ray group.

For example, if a gamma-ray is internally converted, it is sometimes possible to measure the conversion coefficient of this gamma-ray in the K and L shells and the ratio of these two quantities. From this information the multipole order of the radiation and hence the spin and parity change associated therewith can be determined. In addition, if two gamma-rays are emitted in succession, measurement of the angular correlation of the gamma-gamma-coincidences between these two gamma-rays may be made and information concerning the associated angular momentum can be obtained. Experiments have been carried out by Brady and Deutsch (B1, B2) and compared to a theoretical prediction of Hamilton (H2) for the species Co^{60}, Na^{24}, Sc^{46}, Cs^{134}, Rh^{106}, and Y^{88}, from which the angular momenta associated with the several levels have been determined. Finally, a measurement of the shape of the beta-ray spectrum and a computation of the "comparative half-life" (ft-value) will give information on the spin and parity change associated with the beta-ray transition. In most cases the "comparative half-life" gives only an empirical classification (K1) and the spin change determined thereby can only be used as corroborative evidence in case the spins of levels have been determined in some other manner. Within the last year, several examples of a certain type of forbidden beta-ray shape have been discovered by Peacock and Mitchell (P1), Langer and Price (L2), and Shull and Feenberg (S3) which allow one to determine the spin and parity change associated with the beta-ray group concerned. This method has been applied to the interpretation of the spectra of K^{42} (S3) and Cs^{137} (P1). By the use of the above methods, it is sometimes possible, if the spectrum is not too complicated, to assign angular momenta to the various levels of a disintegration scheme.

III. ENERGY LEVEL DIAGRAMS AND DISINTEGRATION SCHEMES

In compiling the energy level diagrams and disintegration schemes given in this section, the author has tried to limit himself to information obtained with the help of beta-ray spectrographs of various types. In most cases presented here, the original investigators measured *both* the gamma-ray spectrum, using a radiator for photo-electrons, *and* the beta-ray spectrum. In no case are schemes included which are based *solely* on absorption measurements or beta-gamma- and gamma-gamma-coincidence measurements. In addition, level schemes arising as a result of cloud-chamber measurements are not considered accurate enough for this survey. In some cases in which the spectroscopic evidence seems good, results of coincidence experiments are cited as confirming the results of the spectroscopic evidence.

There exist in the literature a number of cases in which the beta-ray spectrum of an element, including internal conversion lines, has been investigated by one set of authors, but these authors did not bother to investigate the gamma-rays from a converter. In some cases another group of investigators has measured only the gamma-ray spectrum of the same element. If the

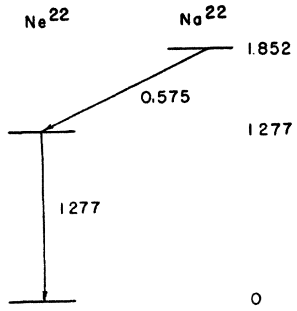

FIG. 1. Energy level diagram of Ne^{22}.

two schemes can be made to agree, the disintegration scheme is usually included, otherwise not. This brings up the question as to what to do about elements formed purely as a result of K-electron capture or lines appearing as a result of K-electron capture. The following are included: (a) Be^7-Li^7, since the levels have been substantiated in other ways; (b) V^{51} has been discussed since several authors agree on the gamma-rays observed but no level scheme has been given; (c) $Co^{56}-Fe^{56}$ has been included since the levels obtained agree well with those from $Mn^{56}-Fe^{56}$; (d) $Mo^{95}-Tc^{95}$, $Tc^{96}-Mo^{96}$ are possibly doubtful cases as stated in the text; (e) $Sn^{113}-In^{113}$ has been well substantiated; (f) Au^{194} and Au^{195} are included to show the relations of the resulting Pt isotopes.

In this section are given the energy levels of 52 product nuclei, together with information on some 60 radioactive transmutations on which these energy levels are based. The information is listed under the symbol of the product nucleus. The radioactive transmutation, or transmutations, together with the decay periods (half-life) from which the information is derived, are also tabulated. Complete disintegration schemes appearing later than July 15, 1949 are not included.

When probable errors are given, these are taken from the original papers. Unfortunately, in the majority of cases, the original papers do not give the probable errors—this is especially true of the older papers. The present author cannot, of course, assign probable errors to other people's work, but he feels, on the basis of his own experience, that, with few exceptions, the probable error of the energies given in this report do not exceed five percent.

The value of the atomic mass of the various radioactive nuclei with respect to the ground state of the product is also given. In those cases in which the mass of the product nucleus is given, the value has been taken from Bethe.*

Li^7

$Be^7 \xrightarrow{K} Li^7$ Period 52.9 d.

Be^7 goes to the ground state and one excited state of Li^7 by the K-capture process. The energy of the excited state is obtained from that of the emitted gamma-ray. Many measurements have been made of the gamma-ray energy, of which the latest show good agreement. These are 0.474±0.004 Mev (Z1), 0.485±0.005 Mev (K2), 0.4767±0.002 Mev (H3), and 0.4785±0.0015 Mev (E1). The branching ratio, i.e., the number of K-captures accompanied by gamma-radiation to the number leading to the ground state is given by Turner (T1) as 0.10 to 0.13.[1] The energy level diagram of Li^7 is given by Lauritsen (L1) in his monograph on the light elements and will not be given here.

Ne^{22}

$Na^{22} \xrightarrow{\beta^+} Ne^{22}$ Period 3.0 yr.

The reaction has been studied by Good, Peaslee, and Deutsch (G2) and earlier by Oppenheimer and Tomlinson (O1). The spectrum consists of one positron group, end-point energy 0.575 Mev, and one gamma-ray of

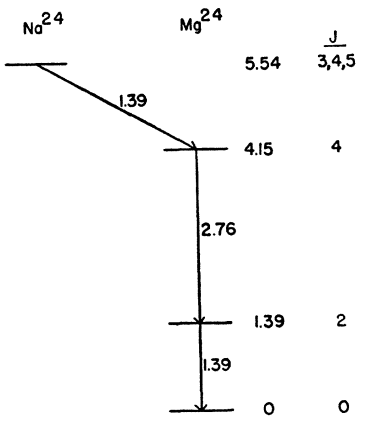

FIG. 2. Energy level diagram of Mg^{24}.

energy 1.30±0.03 Mev as shown in Fig. 1. Alburger (A1) has recently redetermined the energy of the gamma-ray and found 1.277±0.004 Mev for the energy. This value is used in the mass determination given below. The ratio of the number of positrons emitted to the sum of the number of positrons and the number of K-captures $\lambda_+/(\lambda_+ + \lambda_c)$ has been measured by a coincidence counting method (G2) and found to be 1.00 ±0.005. The positron spectrum has an allowed shape. From these latter two pieces of evidence the authors conclude that $\Delta J = 0$ or ± 1 for the positron transition. The comparative half-life is $(ft) = 1.5 \times 10^7$ (K1). The spin[2] of Na^{22} is 3.

$$\text{Mass } Na^{22} = Ne^{22} + 0.003087 = 22.0015.$$

Mg^{24}

$Na^{24} \xrightarrow{\beta} Mg^{24}$ Period 14.8 hr.

This disintegration has been the subject of numerous investigations, the latest of which is by Siegbahn (S4).

* H. A. Bethe, *Elementary Nuclear Theory* (John Wiley and Sons, Inc., New York, 1947).

[1] Recently the branching ratio has been found to be 0.107±0.002 by R. M. Williamson and H. T. Richards, Phys. Rev. **76**, 453 (1949).

[2] L. Davis, Phys. Rev. **74**, 1193 (1948).

He finds one beta-ray group of end-point energy 1.39 Mev and two gamma-rays, of equal intensity, of energies 1.38 and 2.76 Mev. The gamma-ray energies have been redetermined by Robinson, Ter-Pogossian, and Cook, who give 1.380 and 2.765 Mev. The reaction has been the subject of several studies using coincidence counting methods (M1) which show that there is a single beta-ray group followed by the two gamma-rays in cascade. Brady and Deutsch (B2) have measured the angular correlation of the gamma-rays and believe that the spins of the levels are 0, 2, 4 measuring from the ground state up. Konopinski (K1) has made an analysis of the existing beta-ray data and gets the best fit under the assumption that the transition is first forbidden with the vector, tensor, or axial vector interaction. This implies that $\Delta J=0, \pm 1$ (yes). The comparative half-life is $(ft)=12.7\times 10^5$. The disintegration scheme, including possible spins, is given in Fig. 2.

Mass $Na^{24}=Ne^{24}+0.00595=23.9984$.

Al^{27}

$Mg^{27}\xrightarrow{\beta}Al^{27}$ Period 10 min.

This disintegration has been investigated by Benes, Hedgran, and Hole (B3) and by Itoh (I1). There are two beta-ray groups at 1.80 (80 percent) and 0.79 (20 percent) Mev and two gamma-rays at 1.01 and 0.84 Mev. The disintegration scheme is shown in Fig. 3.

Mass $Mg^{27}=Al^{27}+0.00285=26.9928$.

Si^{28}

$Al^{28}\xrightarrow{\beta}Si^{28}$ Period 2.3 min.

This disintegration has been investigated by Benes, Hedgran, and Hole (B3) and by Itoh (I1) using spectrometers. Bleuler and Zünti (B4) have also studied

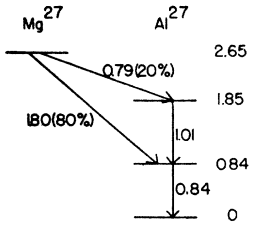

FIG. 3. Energy level diagram of Al^{27}.

the reaction using absorption and coincidence techniques. The disintegration scheme, consisting of one beta-ray of 3.01 Mev followed by one gamma-ray of 1.80 Mev is shown in Fig. 4.

Mass $Al^{28}=Si^{28}+0.00517=27.9918$.

A^{38}

$Cl^{38}\xrightarrow{\beta}A^{38}$ Period 38.5 min.

$K^{38}\xrightarrow{\beta^+}A^{38}$ Period 7.5 min.

The spectrum of Cl^{38} has been studied by a number of investigators, but the most recent and self-consistent results were obtained by Hole and Siegbahn (H4, S5). They find beta-rays of energy 1.19 (36 percent), 2.79 (11 percent), and 5.0 (53 percent) Mev, together with two gamma-rays of energies 1.60 and 2.15 Mev. The disintegration scheme is shown in Fig. 5.

A preliminary investigation of the second reaction has been made, using coincidence counting techniques, by Ramsey, Meem, and Mitchell (R1). They determined a gamma-ray energy of 2.15 Mev, showing that the state of A^{38} at 2.15 Mev is also excited by positron emission.

Mass $Cl^{38}=A^{38}+0.00537=37.979$.

Ca^{42}

$K^{42}\xrightarrow{\beta}Ca^{42}$ Period 12.4 hr.

Siegbahn (S6) and Siegbahn and Johanson (S7) find two beta-rays of energies 2.07 (25 percent) and 3.58 (75 percent) Mev, together with one gamma-ray of 1.51 Mev. In addition to the usual spectroscopic investigation, these authors have made coincidence experiments between the gamma-ray and resolved beta-rays in the spectrograph and have shown that only the low energy beta-ray group is in coincidence with a gamma-ray.

Shull and Feenberg (S3) have reanalyzed the beta-ray data as given by Siegbahn and find that it has a deviation from an allowed shape. The data can be best fitted with a shape factor which corresponds to a first-forbidden spectrum with $\Delta J=\pm 2$ and a change in parity. Since the spin of Ca^{42} is zero, this fixes the angular momentum of K^{42} as $J=2$ with odd parity. The low energy group is then interpreted as first-forbidden with $\Delta J=0$.

The energy level diagram, embodying the results of all of these experiments, is given in Fig. 6.

Mass $K^{42}=Ca^{42}+0.00385=41.9749$.

Ti^{46}

$Sc^{46}\xrightarrow{\beta}Ti^{46}$ Period 85 d.

Meitner (M2), Feister and Curtiss (F1), Miller and Deutsch (M3), and Peacock and Wilkinson (P2) have

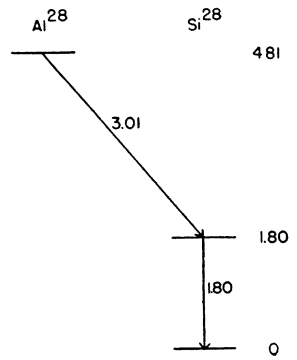

FIG. 4. Energy level diagram of Si^{28}.

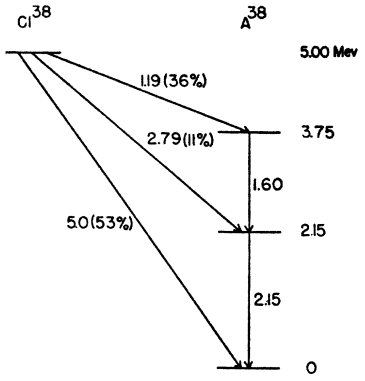

FIG. 5. Energy level diagram of A^{38}.

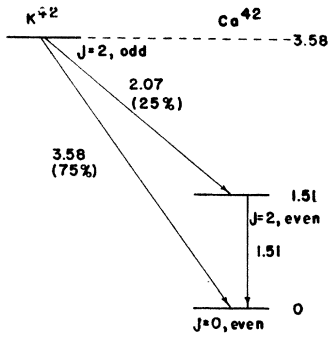

FIG. 6. Energy level diagram of Ca^{42}.

all made measurements on the disintegration scheme of Sc^{46}. The most recent and self-consistent results are due to Peacock and Wilkinson, who find a main group of beta-rays (98 percent) with an end-point energy of 0.36 Mev and in addition a very weak group (2 percent) of much higher energy, 1.49 Mev. Two gamma-rays are found at 0.89 and 1.12 Mev, both of which are internally converted.

The internal conversion coefficients of these two gamma-rays have been measured by Peacock and Wilkinson and found to be $\alpha_K=0.0008$ and 0.0004 for the 0.89-Mev and 1.12-Mev lines, respectively. Comparison of these values with the tables of Rose, Goertzel, Spinrad, Harr, and Strong (R2) shows that the conversion coefficients are consistent with the assumption that each gamma-ray is electric multipole with ΔJ certainly not greater than 3 and probably 2. Brady and Deutsch (B2) have measured the angular correlation of the gamma-rays and attribute angular momenta of 0, 2, 4 to the levels as shown in Fig. 7.

Finally, the (ft) values for the two beta-ray groups are given by Peacock and Wilkinson as 2×10^6 for the low energy transition and 6.8×10^9 for the high energy. The low energy group is presumably first forbidden and the high energy one at least second forbidden.

Mass $Sc^{46}=Ti^{46}+0.00255=45.9686$.

Ti^{48}

$Sc^{48}\xrightarrow{\beta^-}Ti^{48}$	Period 44 hr.
$Va^{48}\xrightarrow{\beta^+}Ti^{48}$	Period 16 d.

The most detailed investigation of the level scheme of Ti^{48} has been made by Peacock and Deutsch (P3) by a study of the disintegration of Va^{48}. The disintegration is accompanied by the emission of one group of positrons of energy 0.716 ± 0.015 Mev followed by two gamma-rays in cascade of energies 0.98 and 1.33 Mev. Robinson, Ter-Pogossian, and Cook (R7) give 0.990 and 1.320 Mev for the energies of these two gamma-rays. Peacock and Deutsch have also made a preliminary investigation of the radiations from Sc^{48}. This element emits the two gamma-rays mentioned above. The beta-ray spectrum has been investigated by Smith (S8) who gives an end point of 0.644 Mev. The Fermi plot, however, is not a straight line, presumably owing to source thickness. The energy level scheme is given in Fig. 7.

It is interesting to note that Pollard (P4) has investigated the ranges of alpha-particles from the reaction $Sc^{45}(\alpha p)Ti^{48}$ and finds Q-values of -0.25, -1.4, -2.6 Mev corresponding to energy levels of 0, 1.15, and 2.25 Mev in excellent agreement with the energy levels determined from radioactive disintegration.

Mass $Sc^{48}=Ti^{48}+0.00316=47.9663$.
Mass $V^{48}=Ti^{48}+0.00435=47.9675$.

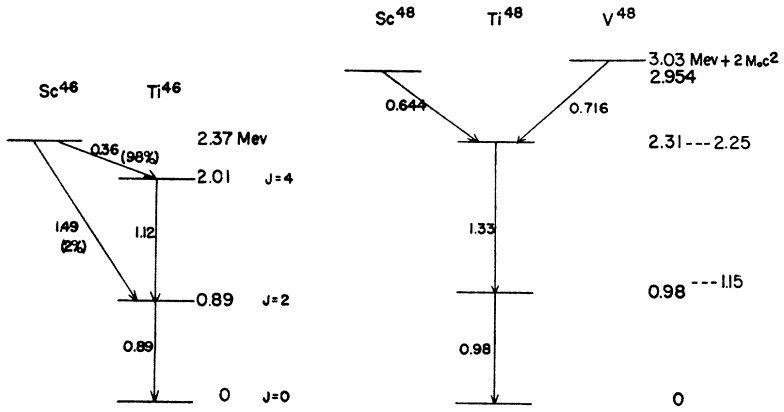

FIG. 7. Energy level diagram of Ti^{46} and Ti^{48}.

V^{51}

$Cr^{51} \xrightarrow{K} V^{51}$ Period 26.5 d.

Of the many investigations of this element, the most recent seem to give a reasonable agreement among themselves. The element decays by K-capture, accompanied by gamma-rays and conversion electrons. Bradt, Gugelot, Huber, Medicus, Preiswerk, and Scherrer (B5) have measured the photo-electrons from a lead radiator and find one gamma-ray of 0.330 ± 0.001 Mev. The electron spectrum shows two internal conversion lines corresponding to gamma-rays of 0.330 and 0.237 ± 0.001 Mev. The second line is entirely converted. Essentially similar results are found by Kern, Mitchell, and Zaffarano (K3) who obtain energies of 0.323 ± 0.005 and 0.267 Mev. The gamma-ray at 0.320 has been noted by Miller and Curtiss (M4), and Kurie and Ter-Pogossian (K2). The disintegration scheme is obviously two gamma-rays in cascade.

Cr^{52}

$Mn^{52} \xrightarrow{\beta^+} Cr^{52}$ Period 6.5 d. and 21 min.

$V^{52} \xrightarrow{\beta} Cr^{52}$ Period 3.9 min.

The isomeric transition of Mn^{52} has been investigated by Peacock and Deutsch (P3) and Osborne and Deutsch (O2) by spectrographic and coincidence techniques. The 6.5-d. isomer emits a positron group of energy 0.582 Mev and three gamma-rays in cascade of energies 0.734, 0.940, and 1.46 Mev. The 21-min. isomer emits a beta-ray of 2.66 Mev followed by the 1.46-Mev gamma-ray. The energy level of the 21-min. state lies 0.400 Mev higher than that of the 6.5-d. isomer, and conversion electrons corresponding to a transition of 0.392 ± 0.008 Mev were found. This definitely establishes that the 1.46-Mev state lies at the bottom of the disintegration scheme.

V^{52} decays to Cr^{52} by electron emission followed by a gamma-ray as has been shown by coincidence counting (P3, R3). Beta-rays of an energy approximately 2.05 Mev and gamma-rays of 1.46 Mev, determined by lead absorption (M5) (B6) are emitted. In addition, conversion electrons from a gamma-ray of 0.250 Mev are present (B6). Work on this isotope is far from conclusive. The main features of the work do show that a 2.05-Mev beta-ray is followed by a gamma-ray of approximately 1.4–1.5 Mev. The internal conversion line at 0.250 Mev is not understood. The disintegration scheme of Mn^{52} together with the main features of that of V^{52} are shown in Fig. 8.

Mass $V^{52} = Cr^{52} + 0.00377 = 51.959$.
Mass $Mn^{52} = Cr^{52} + 0.00509 = 51.961$.

Cr^{54}

$Mn^{54} \xrightarrow{K} Cr^{54}$ Period 310 d.

Mn^{54} decays by K-capture followed by one gamma-ray of 0.835 Mev energy (D3) as shown in Fig. 8.

Fe^{55}

$Co^{55} \xrightarrow{\beta^+ K} Fe^{55}$ Period 18.2 d.

This element decays with approximately equal probability by K-capture and positron emission (D4). It emits two positron groups of energies 1.50 and 1.01 Mev accompanied by three gamma-rays of energies 0.477, 0.935, and 1.41 Mev as shown in Fig. 9. The authors also report a weak gamma-ray at 0.095 Mev which does not fit into the scheme. Table I shows the relative intensities and internal conversion coefficients of the gamma-rays.

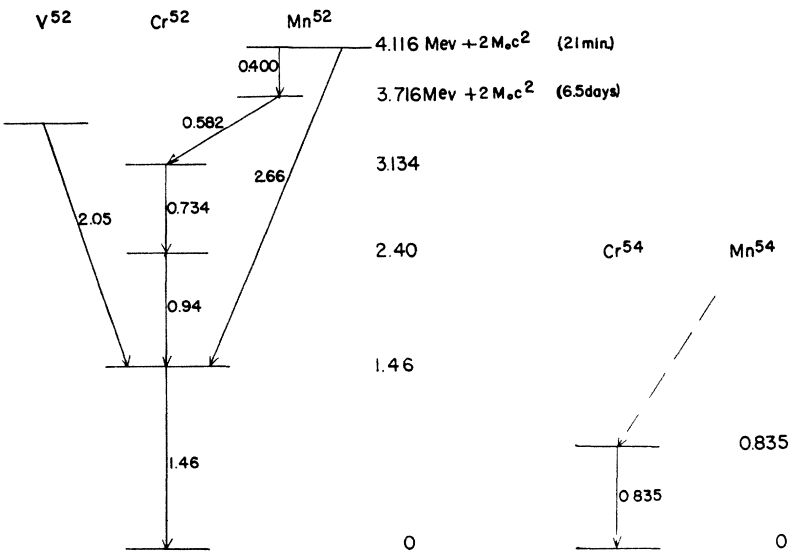

FIG. 8. Energy level diagram of Cr^{52} and Cr^{54}.

TABLE I. Relative intensities and internal conversion coefficients of gamma-rays from $Co^{55} \xrightarrow{\beta^+, K} Fe^{55}$.

Line	Intensity per positron	Internal conversion electrons per positron
0.477	0.3	7.4×10^{-4}
0.935	1.4	5.4×10^{-4}
1.41	0.3	3.5×10^{-5}

Mass $Co^{55} = Fe^{55} + 0.0370$

Fe^{56}

$Mn^{56} \xrightarrow{\beta} Fe^{56}$ Period 2.5 hr.

$Co^{56} \xrightarrow{\beta^+} Fe^{56}$ Period 72 d.

The disintegration of Mn^{56} has been the subject of many studies over a considerable period of time, largely because it can be prepared rather easily and in good strength. Quite good agreement is now obtained for the values of the beta-ray and gamma-ray energies as determined by Elliott and Deutsch (E2) on the one hand, and Siegbahn (S9) on the other. Table II gives a comparison of the energies so obtained and also the values of *ft* for the various beta-ray groups as determined by Siegbahn.

The disintegration has also been the subject of many investigations using coincidence counting methods (M1, E2, S7). As a result of all these investigations, the disintegration scheme given in Fig. 9 is obtained.

The pair nucleus Co^{56} has been studied by Elliott and Deutsch (E2). The fact that it was not possible to prepare this isotope free of other cobalt activities caused considerable trouble in the assignment of various positron groups and gamma-ray lines.

The most energetic positron group has an energy of 1.48 Mev and the Fermi plot is straight down to 0.48 Mev. Below this energy, owing to the presence of other cobalt activities, it is difficult to establish any other positron groups. The authors point out that if low energy groups exist they are of weak intensity. Gamma-rays at 0.845, 1.26, 1.74, 2.01, 2.55, and 3.25 Mev are established by the authors. The higher energy gamma-rays probably occur as a result of orbital electron capture. The line at 0.845 Mev is certainly the same as the one reported in Mn^{56} and the lines at 1.74 and 2.01 Mev are probably the same as similar lines reported in Mn^{56}. The results are shown in Fig. 9, with the line at 3.25 omitted.

TABLE II. Beta- and gamma-ray energies from $Mn^{56} \xrightarrow{\beta} Fe^{56}$.

Reference	Gamma-ray energies (Mev)	Beta-ray energies (Mev)	(*ft*)
E2	0.85, 1.81, 2.13	0.75, 1.05, 2.86	
S9	0.822, 1.77, 2.06	0.75, 1.04, 2.81	0.95×10^4, 0.40×10^6, 13.2×10^6
Rel. int.		(20%) (30%) (50%)	

Mass $Mn^{56} = Fe^{56} + 0.00390 = 55.9607$.
Mass $Co^{56} = Fe^{56} + 0.00495 = 55.9618$.

Fe^{58}

$Co^{58} \xrightarrow{\beta^+K} Fe^{58}$ Period 72 d.

Co^{58} decays by *K*-capture and positron emission accompanied by the emission of one gamma-ray. Deutsch and Elliott (D3) give the energy of the positron as 0.47 Mev and the gamma-ray as 0.805 Mev. (See Fig. 9.) The number of positrons emitted per disintegration is 0.145 ± 0.005 (G2).

Mass $Co^{58} = Fe^{58} + 0.002467$.

Co^{59}

$Fe^{59} \xrightarrow{\beta} Co^{59}$ Period 47 d.

The disintegration of Fe^{59}, investigated by Deutsch, Downing, Elliott, Irvine, and Roberts (D14), is accompanied by the emission of two beta-ray groups, of approximately equal intensity, of energies 0.260 and

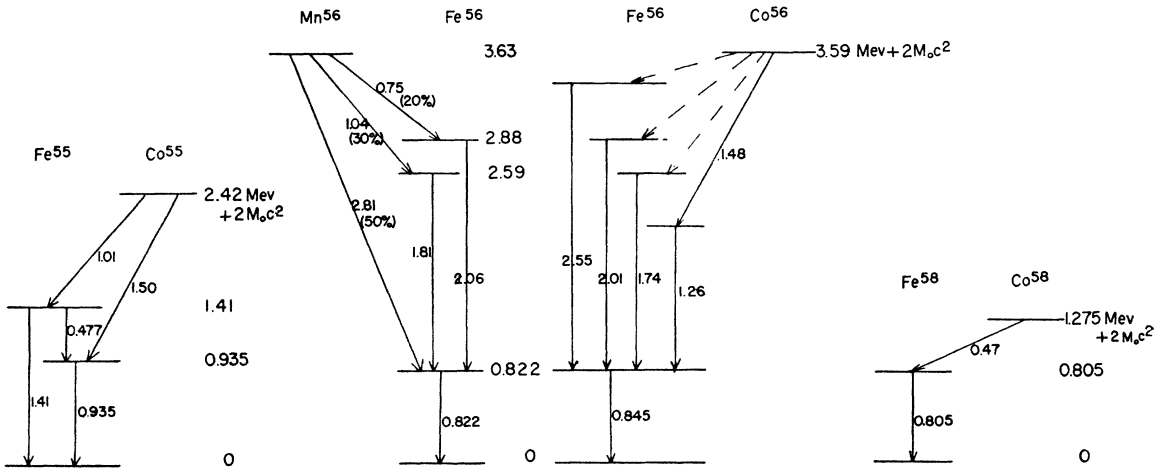

FIG. 9. Energy level diagram of Fe^{55}, Fe^{56}, and Fe^{58}.

0.460 Mev, together with two gamma-rays of 1.10 and 1.30 Mev. The level scheme is shown in Fig. 10.

Mass $Fe^{59} = Co^{59} + 0.00168$.

Ni^{60}

$Co^{60} \xrightarrow{\beta} Ni^{60}$ Period 5.3 yr.

Isomeric period 10.7 min.

The isomeric transitions of Co^{60} (10.7 min. and 6.3 yr.) have been investigated by Deutsch, Elliott, and Roberts (D5). The 5.3-yr. isomer emits one beta-ray of 0.308 Mev followed by two gamma-rays of energy approximately 1.10 and 1.30 Mev in cascade. More recent work of Jensen, Laslett, and Pratt (J1, J5), Alburger (A1), and Lind, Brown, and DuMond (L7), using a crystal spectrometer, yields the values listed below:

Reference	Energy
J1	1.156; 1.317
J5	1.169; 1.331
A1	1.175±0.006; 1.332±0.005
L7	1.1715±0.0010; 1.3316±0.0010.

The crystal spectrometer values of Lind, Brown, and DuMond are the most accurately determined. As a result of angular correlation experiments (B2) spins of 0, 2, 4 are assigned to the three levels in question.

Deutsch, Elliott, and Roberts also made measurements on the 10.7-min. isomer. Owing to the short period and probably to the relatively low specific activities available at that time, they were not able to make as accurate spectroscopic investigations as they did on the longer lived isomer. They report an internal conversion line corresponding to a gamma-ray whose energy is 0.056±0.003 Mev. They give the beta-ray end point as 1.28±0.06 Mev. Their coincidence studies show that the beta-ray is in coincidence with a gamma-ray of about 1.5 Mev. Their original scheme shows a level at 1.30 Mev above the ground state of Ni^{60} fed by gamma-rays from the long-lived isomer and, in addition, a level at 1.45 Mev fed by a beta-ray from the short-lived isomer. The recent spectroscopic determination of Peacock, Jones, and Overman (P18) gives a beta-ray end point for the 10.7-min. isomer of 1.56 Mev. As a result of these new measurements, it appears that the extra level at 1.45 Mev, originally postulated by Deutsch, Elliott, and Roberts coincides with that at 1.332.

The level scheme is given in Fig. 11.

Mass $Co^{60} = Ni^{60} + 0.0030193 = 59.9525$.

Cu^{65}

$Zn^{65} \xrightarrow{K\beta^+} Cu^{65}$ 250 d.

$Ni^{65} \xrightarrow{\beta} Cu^{65}$ 2.6 hr.

The most extensive work on the levels of Cu^{65} comes from the disintegration of Ni^{65} studied by Siegbahn and Ghosh (S23) who find three beta-ray groups at 2.10 (57 percent), 1.01 (14 percent), and 0.60 (29 percent) Mev together with three gamma-rays at 1.12, 1.49, and 0.37 Mev. These results lead to the scheme shown in Fig. 12. A check on this scheme by coincidence counting methods has been obtained by Maienschein and Meem (M6).

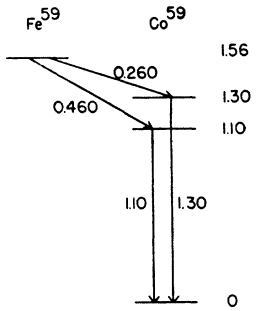

FIG. 10. Energy level diagram of Co^{59}.

Zn^{65} appears to emit only one gamma-ray of energy 1.118 Mev (J5) accompanied by a positron of 0.32 Mev (P5) and orbital electron capture.

Mass $Ni^{65} = Cu^{65} + 0.00226 = 64.9573$.
Mass $Zn^{65} = Cu^{65} + 0.00264 = 64.9576$.

Ge^{72}

$Ga^{72} \xrightarrow{\beta} Ge^{72}$ Period 14.1 hr.

The spectrum of Ga^{72} is extremely complicated but Mitchell, Zaffarano, and Kern (M7) on the one hand, and Haynes (H5) on the other, have obtained results which are in essential agreement. There are seven beta-ray groups of energies 3.17 (8 percent), 2.57 (8 percent), 1.74 (3 percent), 1.45 (7 percent), 1.00 (26 percent), 0.74 (23 percent), and 0.56 (25 percent) Mev. The gamma-ray energies are 0.835, 0.631, 0.691 (1.05, 1.30, 1.47, 1.57), 1.81, 2.18, and 2.50 Mev, those given in parentheses being weak. The energy of the stronger gamma-rays has been determined to one percent. The over-all agreement in adding up the energies by various routes is

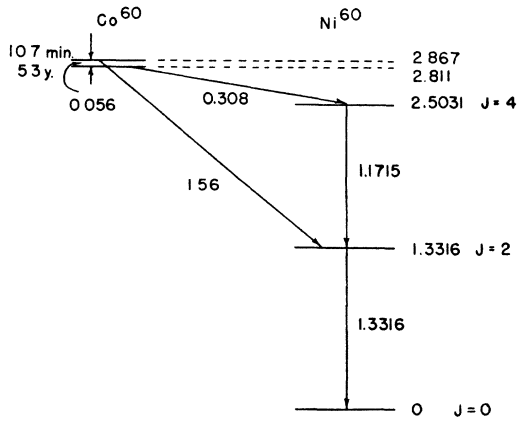

FIG. 11. Energy level diagram of Ni^{60}.

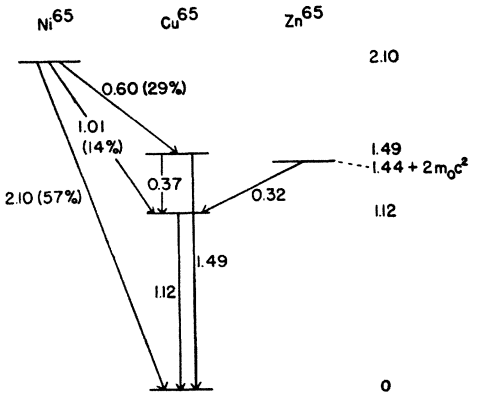

FIG. 12. Energy level diagram of Cu^{65}.

to better than five percent. A reasonable disintegration scheme is shown in Fig. 13.

Mass $Ga^{72}=Ge^{72}+0.00431$.

Se^{76}

$As^{76}\xrightarrow{\beta}Se^{76}$ Period 26.75 hr.

Most of the earlier work on this element, on which there are a number of papers, suffered from weak sources and low resolving power instruments. The most recent work of Siegbahn (S11) gives a self-consistent scheme (Fig. 14), consisting of three beta-ray groups at 1.29 (15 percent), 2.49 (25 percent), and 3.04 (60 percent) Mev and three gamma-rays at 1.75, 1.20, and 0.55 Mev.[3]

Mass $As^{76}=Se^{76}+0.00327$.

Kr^{82}

$Br^{82}\xrightarrow{\beta}Kr^{82}$ Period 34 hr.

The spectrum of Br^{82} was originally worked out by Roberts, Downing, and Deutsch (R6) in 1941. They found one beta-ray group of energy 0.465 Mev and three gamma-rays of energy 0.547, 0.787, and 1.35 Mev. In the intervening eight years, instruments and techniques have improved greatly and, as a result, recent work of Siegbahn (S10) has shown the scheme to be much more complicated. He has found three beta-ray groups at 0.447, 0.323, and 0.181 Mev. In addition, there are six gamma-rays,[4] all internally converted, of energies 1.321, 0.769, 1.036, 0.610, 0.652, and 0.550 Mev. He gives the scheme shown in Fig. 15 which,

[3] The recent work of Marty, Labeyrigue, and Langevin, Comptes Rendus **228**, 1722 (1949), throws some doubt on the scheme presented in Fig. 14. They found beta-rays with end-point energies (in Mev) at 3.15 (54 percent), 2.56 (21 percent), 1.4 (19 percent), and 0.4 (7 percent). Gamma-rays at 0.56 and 1.25 Mev were the only ones found. Clearly the work of these authors is incomplete since it does not present a consistent scheme, but the presence of the low energy group should be reinvestigated.

[4] Dr. Siegbahn writes that he has found an additional gamma-ray and the scheme may have to be revised.

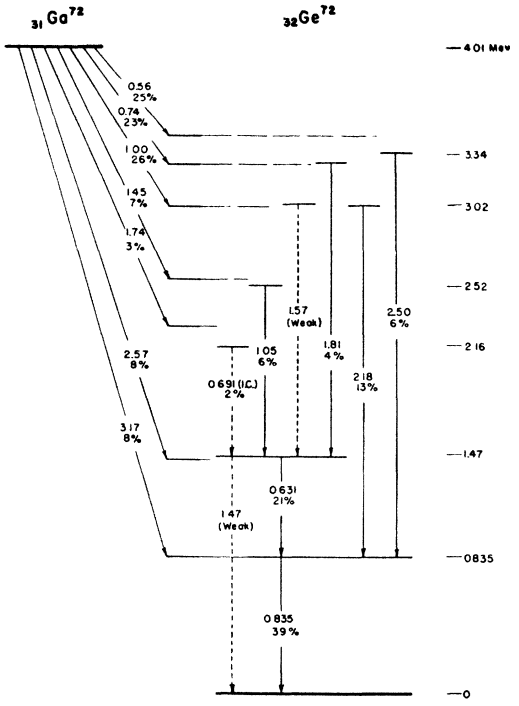

FIG. 13. Energy level diagram of Ge^{72}.

it is understood, may have to undergo revision.

Mass $Br^{82}=Kr^{82}+0.003838$.
Mass† $Br^{82}=81.942$.

Sr^{86}

$Rb^{86}\xrightarrow{\beta}Sr^{86}$ Period 19.5 d.

The spectrum of Rb^{86} has been worked out by Zaffarano, Kern, and Mitchell (Z2), who find the spectrum to consist of two beta-ray groups with end points at 0.716 ± 0.02 (20 percent) and 1.822 ± 0.014 (80 percent) Mev. There is only one gamma-ray of energy 1.081 ± 0.006 Mev. The disintegration scheme is shown in Fig. 16. The shape of the beta-ray distribution for the high energy group can be fitted with a shape factor which corresponds to a first-forbidden transition with $\Delta J=\pm2$. Since the spin of Sr^{86} is zero, the spin of Rb^{86} is probably 2 and that of the excited level of Sr^{86} is

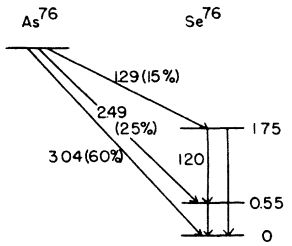

FIG. 14. Energy level diagram of Se^{76}.

† Mass of Kr^{82} taken from Mattauch and Flügge, *Nuclear Physics Tables* (Interscience Publishers, Inc., New York, 1946).

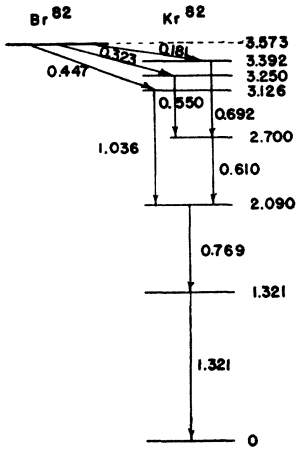

FIG. 15. Energy level diagram of Kr^{82}.

probably 1. The decay scheme has been substantiated by Jurney (J2) using coincidence counting methods.

Mass $Rb^{86} = Sr^{86} + 0.002011$.

Sr^{88}

$Y^{88} \xrightarrow{K\beta^+} Sr^{88}$ Period 105 d.

The spectrum as originally reported by Downing, Deutsch, and Roberts (D6), consisted of two gamma-rays at 0.908 and 1.89 Mev and no positrons. Recently Peacock and Jones (P6) have reported the gamma-rays as 0.908, 1.853, and 2.76 Mev. In addition, they reported a positron group at 0.83 Mev. The disintegration scheme is given in Fig. 16.

Mass $Y^{88} = Sr^{88} + 0.00495$.

Cb^{95}; Mo^{95}

$$Zr^{95} \xrightarrow[65\text{ d.}]{} Cb^{95} \xrightarrow[90\text{ hr.}]{53\text{ d.}} Mo^{95}$$

$Tc^{95} \xrightarrow{K\beta^+} Mo^{95}$ Period 62 d.

The spectrum of Te^{95} has been investigated by Huber, Medicus, Preiswerk, and Steffen (H6). They have published a decay scheme for Te^{95} which is shown in Fig. 17. Since the only positron group emitted goes to the ground state, there is no possibility of checking the energy levels by means of positron group end points. The, at present, fragmentary information existing on the $Zr^{95} \rightarrow Cb^{95} \rightarrow Mo^{95}$ chain (S1, H7) does not seem to fit into this scheme.

Mo^{96}

$Tc^{96} \xrightarrow{K} Mo^{96}$.

A rather complicated scheme, Fig. 17, is given by Medicus, Mukerji, Preiswerk, and de Saussure (M18). Here again, as in Mo^{95}, there is no possibility of checking levels by beta-ray groups.

Pd^{106}

$$Ru^{106} \xrightarrow[330\text{ d.}]{} Rh^{106} \xrightarrow[30\text{ sec.}]{} Pd^{106}.$$

Peacock (P7) has investigated the spectrum of Rh^{106} (30 sec.) and finds two beta-ray groups at 3.55 (82 percent) and 2.30 (18 percent) Mev, accompanied by three gamma-rays at 0.51, 0.75, and 1.25 Mev. He states that the beta-rays from Ru^{106} are of such low energy as not to disturb the measurements. Peacock (P7) and also Jurney (J3) have confirmed the scheme given in Fig. 18 by coincidence counting methods.

Pd^{106} can also be formed from Ag^{106} which has been investigated by Enns (E3) and Deutsch, Roberts, and Elliott (D7). Since the results of these two papers are not in complete agreement with each other, they are omitted here.

Mass $Rh^{106} = Pd^{106} + 0.00381 = 105.9448$.

Cd^{110}

$Ag^{110} \xrightarrow{\beta} Cd^{110}$ Period 225 d. and 24 sec.

Fragmentary information on the very complicated decay scheme of the Ag^{110} isomers has been supplied by a number of authors (E4, D7, D8, R4) but the detailed scheme has been worked out by Siegbahn (S12).

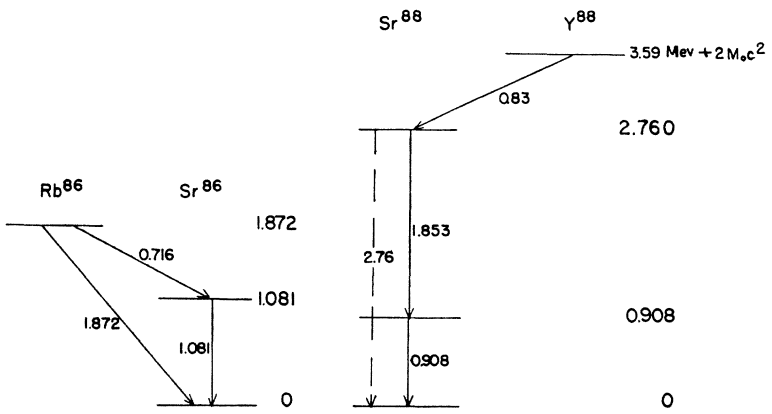

FIG. 16. Energy level diagram of Sr^{86} and Sr^{88}.

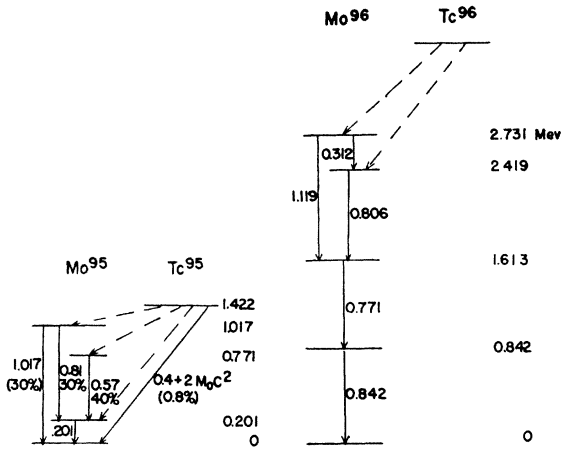

FIG. 17. Energy level diagram of Mo^{95} and Mo^{96}.

In all, ten gamma-rays are found at 0.116, 0.656, 0.676, 0.706, 0.759, 0.814, 0.885, 0.935, 1.389, and 1.516 Mev. Three main beta-ray groups are found at 2.86, 0.530, and 0.087 Mev, together with indications of some weaker groups. The decay scheme is given in Fig. 19.

Mass $Ag^{110}=Cd^{110}+0.00307$.

Cd^{111}

$Cd^{111m}\rightarrow Cd^{111}$.

This metastable state is produced by fast neutrons on Cd (D9) and also by the action of x-rays and electrons on Cd (W1, W2). The spectrum has been measured by Hole (H8) who finds two conversion lines associated with gamma-rays at 0.145 and 0.230 Mev. He also finds the higher energy line from an investigation of the photo-electrons produced in a lead radiator. The disintegration scheme is given in Fig. 20, but the order of emission of the gamma-rays is not known.

In^{113}

$Sn^{113}\xrightarrow{K}In^{113m}$ Period 105 d.

$In^{113m}\rightarrow In^{113}$ Period 105 min.

Barnes (B11) has shown that Sn^{113} decays by K-capture to a In^{113} which goes with the emission of a converted gamma-ray of energy 0.085 Mev to In^{113m}. This decays with the emission of a converted gamma-ray of 0.392 Mev to the ground state of In^{113}. The scheme is shown in Fig. 21.

In^{115}

$Cd^{115}\xrightarrow{\beta}In^{115m}\rightarrow In^{115}$ Period 56 hr. and 4.5 hr.

Cd^{115} disintegrates to In^{115m} with a period of 56 hr. which then goes to In^{115} with a period of 4.5 hr. These transitions have been investigated by Lawson and Cork (L3) using a spectrometer. They find two beta-ray groups at 0.6 and 1.13 Mev and a gamma-ray of 0.54 Mev associated with the 56-hr. period and an internally converted gamma-ray of 0.338 Mev associated with the 4.5-hr. metastable state. The results are shown in Fig. 21.

Mass $Cd^{115}=In^{115}+0.00158$.

Sn^{116}

$In^{116}\xrightarrow{\beta}Sn^{116}$ Period 54 min.

Some preliminary work has been done on the element by Curtis and Richardson (C1) who used a cloud chamber to measure both the energy of the beta-rays and the gamma-rays. Some preliminary work on the energy of the gamma-rays has been reported by Deutsch, Roberts, and Elliott (D7) but at the present time no complete disintegration scheme can be given.

Te^{122}

$Sb^{122}\xrightarrow{\beta}Te^{122}$ Period 2.6 d.

The spectrum of this element, usually occurring with Sb^{124} (60 d.) has been investigated in a spectrometer by a number of people. Miller and Curtiss (M8) give the beta-ray energies as 1.94 and 1.36 Mev. The gamma-ray energy has been measured by Rall and Wilkinson (R4), Kern, Zaffarano, and Mitchell (K4), and Cook and Langer (C2), and has the value 0.568 Mev. The scheme is shown in Fig. 22.

Mass $Sb^{122}+Te^{122}=0.00208$.

Te^{124}

$Sb^{124}\xrightarrow{\beta}Te^{124}$ Period 60 d.

$I^{124}\xrightarrow{\beta+K(?)}Te^{124}$ Period 4 d.

The spectrum of Sb^{124} has been the subject of investigation by various authors over a period of years. Most of these investigations were not successful, however, in

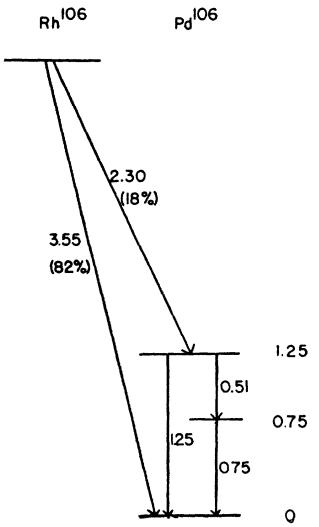

FIG. 18. Energy level diagram of Pd^{106}.

obtaining a complete picture of this rather complicated scheme.[5] The complete scheme has been worked out by Kern, Mitchell, and Zaffarano (K4) and by Cook and Langer (C2). There are five beta-ray groups at 2.37 (21 percent), 1.62 (8 percent), 1.00 (9 percent), 0.65 (44 percent), and 0.48 (18 percent) Mev. Gamma-rays at 2.056±0.05, 1.708±0.02, 0.714±0.02, 0.650 ±0.05, and 0.603±0.002 Mev have been found. The line at 0.603 Mev is internally converted. In addition there is another internal conversion line corresponding to a gamma-ray at 0.121 Mev (C2). The agreement between the two groups is remarkably good. The values given here are those of K4.

The spectrum of the 4-d. positron emitter I^{124} has been investigated by Mitchell, Mei, Maienschein, and Peacock (M11) who find the lines at 0.603 (internally converted), 1.715, 1.95, and a weak line at about 0.730 Mev. Three groups of positrons at 2.20±0.02 (51 percent), 1.50±0.02 (43 percent), 0.68±0.05 (5 percent) Mev are also found. These data fit in quite well with the results obtained on Sb^{124}. The results are shown in Fig. 22.

The disintegration scheme of Sb^{124} has also been investigated by coincidence counting methods (M9, M10, W3, J4), the most recent work (J4) giving a reasonable check on the scheme proposed in Fig. 22.

Mass $Sb^{124}=Te^{124}+0.00319$.
Mass $I^{124}=Te^{124}+0.00411$.

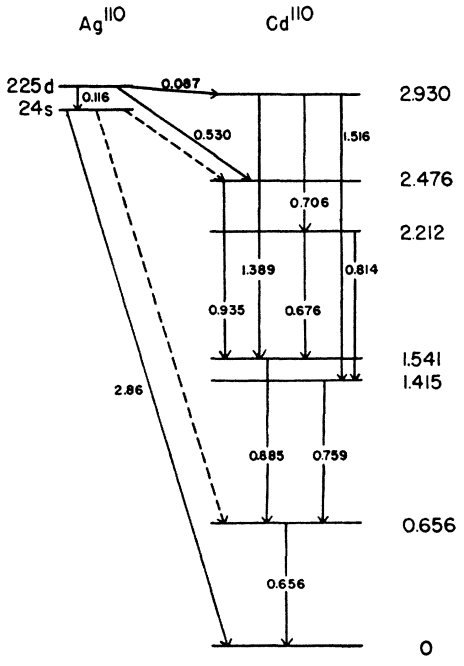

FIG. 19. Energy level diagram of Cd^{110}.

[5] For a summary of the earlier investigations the reader should see S1.

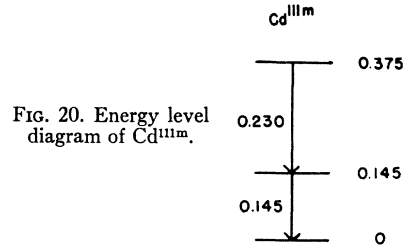

FIG. 20. Energy level diagram of Cd^{111m}.

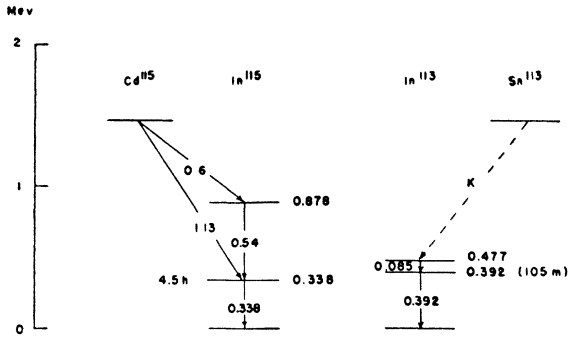

FIG. 21. Energy level diagram of In^{113} and In^{115}.

Te^{125}

$Sb^{125} \xrightarrow{\beta} Te^{125}$ Period 2.7 yr.

Sb^{125} grows from a short-lived Sn^{125} (9 min.). Among the products of its rather complicated decay scheme is the long-lived metastable state of Te^{125} (60 d.). The disintegration has been investigated by Kern, Mitchell, and Zaffarano (K3) on the one hand, and by Siegbahn (S13) on the other. Some of the gamma-rays were observed as conversion lines, some as photo-lines from a lead radiator and some as both. The results are given in Table III. In Table III the method of detection is that employed in K3. The beta-ray groups as given by the two sets of investigators are also given in Table III. The values of the relative abundance of the beta-rays are those of Siegbahn. The strongest gamma-rays are those at 0.431, 0.609, and 0.174 Mev, while the lines at 0.646, 0.466, and 0.125 are considerably weaker.

The metastable state Te^{125m} (60 d.), discovered by Friedlander, Goldhaber, and Scharf-Goldhaber (F2), decays with the emission of a converted gamma-ray of 0.110 Mev and one of 0.035 Mev (H10, K3, S13). The ratio N_K/N_L for the 0.110 line is 1.2, which indicates that the transition associated with this line is mostly magnetic 2^4 pole radiation (D10).

Probably the best disintegration scheme is that due to Siegbahn which is shown on Fig. 22. This scheme does not include the weak line at 0.125.

Mass $Sb^{125}=Te^{125}+0.00081$.

Xe^{126}

$I^{126} \xrightarrow{\beta} Xe^{126}$ Period 13 d.

This disintegration has been measured by Mitchell, Mei, Maienschein, and Peacock (M11) with a source

TABLE III. Sb^{125}.

Element	How detected	*KMZ* energy Mev	*S*
	Gamma-rays		
Te	IC	—	0.035
Te	IC	0.110±0.001	0.110
Sb	IC	0.125±0.001	—
Sb	IC; photo	0.174±0.002	0.175
Sb	IC; photo	0.431±0.004	0.425
Sb	Photo	0.466±0.006	0.465
Sb	IC; photo	0.609±0.006	0.601
Sb	Photo	0.646±0.009	0.637

Beta-rays

KMZ	*S*	Abundance (percent)
0.621 Mev	0.616 Mev	18
0.288	0.299	49
—	0.128	33

which also gave I^{124}. There are two beta-ray groups at 1.268±0.01 (27 percent) and 0.85±0.05 (73 percent) accompanied by a gamma-ray of energy 0.395±0.005 as shown in Fig. 23. The gamma-ray is internally converted.

Mass $I^{126}=Xe^{126}+0.00136$.

Xe^{128}

$I^{128}\xrightarrow{\beta}Xe^{128}$ Period 25 min.

This isotope has been studied by Siegbahn and Hole (S14). The decay occurs mostly by a direct beta-ray transition to the ground state—2.02 Mev (93 percent)—accompanied by a weaker transition of lower energy—1.59 Mev (7 percent)—to an excited state from which a gamma-ray of 0.428±0.002 Mev is emitted. The scheme is shown in Fig. 23. The authors give the following *ft*-values for the two groups: $(ft)_1=4.1\times10^6$, $(ft)_2=0.78\times10^6$.

Mass $I^{128}=Xe^{128}+0.00217$.

Xe^{130}

$I^{130}\xrightarrow{\beta}Xe^{130}$ Period 12.6 hr.

The 12.6-hr. I^{130} has been investigated by Roberts, Elliott, Downing, Peacock, and Deutsch (R5). They find two beta-ray groups at 0.61±0.02 (40 percent) and 1.03±0.02 (60 percent) Mev. Gamma-rays of energies 0.417±0.008, 0.537±0.005, 0.667±0.008, and 0.744 ±0.010 Mev are present and all four are internally converted. The disintegration scheme is given in Fig. 23. It will be noticed that only the line at 0.417 Mev can be definitely placed, from the evidence of the two beta-ray groups. The position of the remaining three gamma-rays is entirely arbitrary. The authors have substantiated this scheme by coincidence counting techniques.

Mass $I^{130}=Xe^{130}+0.00319$.

Xe^{131}

$I^{131}\xrightarrow{\beta}Xe^{131}$ Period 8.0 d.

This disintegration has been the subject of several investigations. The earlier work of Downing, Deutsch, and Roberts (D11) was done with such a weak source that only an incomplete disintegration scheme was obtained. Work completed during the last year by Metzger and Deutsch (M12), Kern, Mitchell, and Zaffarano (K3), Owen, Moe, and Cook (O3, M13), together with the wave-length determination by DuMond and his co-workers (L4) has led to a considerably better understanding of the scheme.

The energies of the main gamma-rays are (K3):[6] 80±2, 282±1, 363±2, 637±2 kev. The results of the other workers who used magnetic spectrographs are in agreement with these values. The crystal method gives the values 80.133±0.005, 284.13±0.1, 364.18±0.1 kev, the high energy gamma-ray not being measured. The three low energy lines are internally converted. There is some question as to whether the one at 637 kev is converted. In addition, there is evidence of a weak gamma-ray, also converted, at 163 kev (K3, O3, M13).

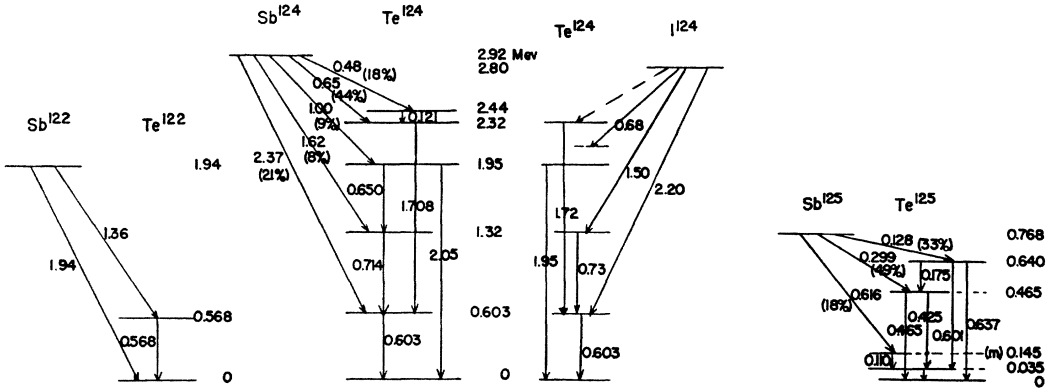

FIG. 22. Energy level diagram of Te^{122}, Te^{124}, and Te^{125}.

[6] The energies are given here in kev instead of Mev since the values obtained with the crystal spectrometer are given in these units.

This line appears to be due to a metastable state of Xe^{131} (B7). At the present time it does not seem to be possible to fit this line into the decay scheme. The intensities and internal conversion coefficients of the three low energy lines are given in Table IV.

The beta-ray spectrum may be decomposed into two groups of energies: 605±5 kev (86 percent) and 250 ±30 kev (14 percent) (K3).

The most plausible disintegration scheme, leaving out the line at 163 kev, is shown in Fig. 23.

Mass $I^{131}=Xe^{131}+0.00104$.

Ba^{134}

$Cs^{134}\xrightarrow{\beta}Ba^{134}$ Period 1.7 yr.

This element, originally investigated by Siegbahn and Deutsch (S15, S16), has been completely worked out by Elliott and Bell (E5). Gamma-rays occur at 0.568 ±0.015, 0.602±0.015, and 0.794±0.015 Mev of relative intensities 0.26, 1.00, and 1.00. There is some evidence for a very weak line at 1.35 Mev. Beta-rays occur at 0.658±0.030 (75 percent) and 0.090 Mev (25 percent). The scheme is shown in Fig. 24. Coincidence experiments by the above authors and Meem and Maienschein (M14) have given full confirmation to the scheme.

Mass $Cs^{134}=Ba^{134}+0.00221$.

Ba^{137}

$Cs^{137}\xrightarrow{\beta}Ba^{137m}\longrightarrow Ba^{137}$ Period 33 yr.

This element has been the subject of several investigations starting with that of Townsend, Owen, Cleland, and Hughes (T2), who found one beta-ray group of energy 0.550 Mev and an internally converted gamma-ray of energy 0.665±0.005 Mev. They also discovered a metastable state of Ba^{137} (T3) of half-life 156 sec. Mitchell and Peacock (M15, P1) have reinvestigated the spectrum. They find that the main beta-ray group (95 percent) has a forbidden shape characterized by $\Delta J=\pm 2$, change of parity, first forbidden, whose end point is 0.531±0.005 Mev. In addition, they find a weak (5 percent) group of higher energy, approximately 1.19 Mev, which is probably third forbidden. The value of (ft) for the two groups are: $(ft)_{0.531}=2.3\times10^{9}$ and $(ft)_{1.19}=1.4\times10^{12}$. These results are confirmed by Osaba.[7]

Mitchell and Peacock have also measured the internal conversion coefficient α_K and the ratio N_K/N_L. From these values and the known half-life of Ba^{137m}, they conclude that the spin change in the transition $Ba^{137m}\longrightarrow Ba^{137}$ is 5 units. From these considerations, and from arguments based on the shape of the beta-ray spectrum, reasonable values for the spin changes in all the transitions may be obtained. Since the spin of Ba^{137} is known to be 3/2, the spins[7] of the other states can be computed. The energy level diagram is given in Fig. 24.

Mass $Cs^{137}=Ba^{137}+0.00128$.

La^{140}

$Ba^{140}\xrightarrow{\beta}La^{140}$ Period 12.8 d.

Fragmentary information on the decay of Ba^{140} and that of its daughter substance La^{140} has been in existence for some time (R4, O4, M4), but the complete

TABLE IV. Intensities and internal conversion in I^{131}.

Energy of gamma-ray kev	Intensity, quanta per 100 disintegrations	Conversion coefficient $Ne/N\gamma$	N_K/N_L
80	17.9	0.17	8.4
282	14.2	0.079	—
363	82.5	0.018	4.0

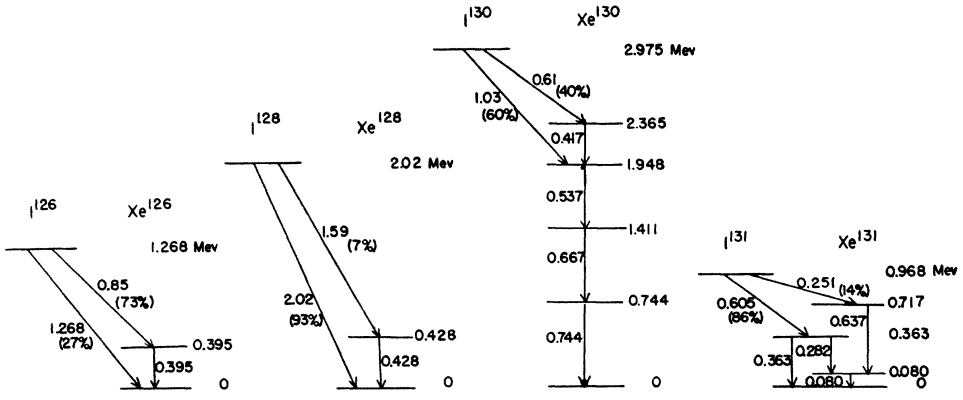

FIG. 23. Energy level diagram of Xe^{126}, Xe^{128}, Xe^{130}, and Xe^{131}.

[7] The spectrum of Cs^{137} has been reinvestigated by J. S. Osaba [Phys. Rev. **76**, 345 (1949)] who is in general agreement with Mitchell and Peacock on the energy aspects of the spectrum. His value for the internal conversion coefficient is lower than that of Mitchell and Peacock, and he suggests that the spin change accompanying the gamma-ray is four units. This would make the spin of Ba^{137m} 11/2 and that of Cs^{137} 7/2. The spin of Cs^{137} has been determined by L. Davis, Jr. [Phys. Rev. **76**, 435 (1949)] and D. E. Nagle [Phys. Rev. **76**, 847 (1949)] who find its value to be 7/2.

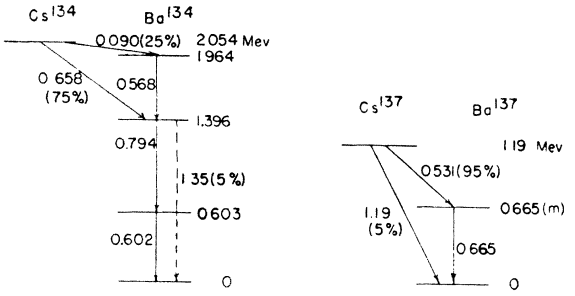

FIG. 24. Energy level diagram of Ba^{134} and Ba^{137}.

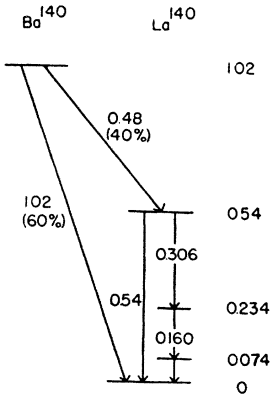

FIG. 25. Energy level diagram of La^{140}.

decay scheme has only now been completed. Beach, Peacock, and Wilkinson (B8) have given self-consistent schemes for both Ba^{140} and La^{140}. The spectrum of Ba^{140} consists of two beta-ray groups at 1.022 (60 percent) and 0.48 (40 percent) Mev together with three gamma-ray lines, all internally converted, at 0.160, 0.306, 0.540 Mev. The disintegration scheme is given in Fig. 25.

Mass $Ba^{140}=La^{140}+0.00109$.

Ce^{140}

$La^{140}\xrightarrow{\beta}Ce^{140}$ Period 40 hr.

The same authors (B8) have measured the disintegration scheme of La^{140}. They find beta-ray groups at 2.26 (10 percent), 1.67 (20 percent), and 1.32 (70 percent) Mev and gamma-rays at 2.5, 1.62, 0.82, 0.49, 0.335, and 0.093 Mev. The lines at 0.49, 0.335, and 0.093 are converted. The strong line in the spectrum is that at 1.62 Mev while the line at 2.5 Mev is so weak that no photo-electrons are found. Its energy is determined from the shape of the Compton-electron curve. The decay scheme is given in Fig. 26.

Mass $La^{140}=Ce^{140}+0.00411$.

Ho^{165}

$Dy^{165}\xrightarrow{\beta}Ho^{165}$ Period 2.5 hr.

The investigation of this element presents difficulties since the gamma-radiation is quite weak compared to the beta-radiation. An investigation has been carried out in a magnetic lens spectrometer by Slätis (S17). He finds three beta-ray groups at 1.28±0.02, 0.88, and 0.42 Mev, accompanied by three gamma-rays of energies 0.76±0.07, 0.37±0.02, and 0.091 Mev. The disintegration scheme is given in Fig. 27. Here an additional beta-ray group, not found, is shown by the dotted line. This is done to account for the presence of the gamma-ray at 0.091 Mev.

Mass $Dy^{165}=Ho^{165}+0.00137$.

Yb^{170}

$Tm^{170}\xrightarrow{\beta}Yb^{170}$ Period 127 d.

Saxon and Richards (S18), Graham and Tomlin (G3), Grant and Richmond (G4), Agnew (A2), and Fraser (F3) have measured the spectrum of Tm^{170}. In addition, Grant and Richmond (G4), Graham and Tomlin (G3), Kettelle (K5), and Fraser (F3) have made coincidence studies on the beta-rays and gamma-rays, or x-rays and gamma-rays, emitted during the disintegration. There is some disagreement between the various authors. All are agreed, however, that there is a highly internally converted gamma-ray at approximately 84 kev. The values given are (in kev) 85.5±0.5 (S18), 85.4±0.6 (A2), 83.9 ±0.2 (F3), 82.7±? (G3), 82.6±0.7 (G4).

Two of the authors (F3) and (G3) attempted to find other gamma-rays by using a source with a lead radiator but found no other gamma-rays.

All of the authors who have investigated the beta-rays agree that the Fermi plot of the beta ray-spectrum does not give a good straight line. Agnew has attempted to fit various shape factors to the data but could find none which would give a fit. Fraser has been able to analyze the spectrum into two groups of end-point energies at 0.886±0.005 Mev (10 percent) and 0.970 ±0.005 Mev (90 percent). The remaining authors with the exception of Grant and Richmond give an end-point energy of 0.970±0.010 Mev. From the coincidence

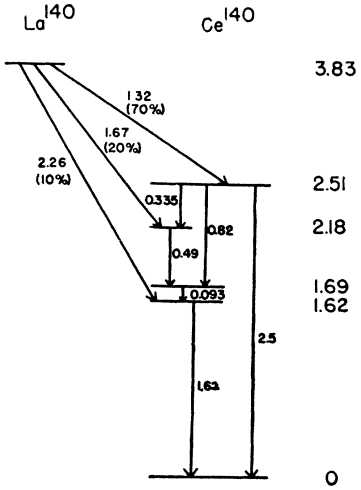

FIG. 26. Energy level diagram of Ce^{140}.

experiments of Fraser (F3) and Kettelle (K3), it appears likely that the spectrum consists of two groups of beta-rays at 0.886 and 0.970 Mev and one gamma-ray at 0.084 Mev.

The paper of Grant and Richmond is so brief that no opinion can be formed of the experiments they performed. They report beta-rays at 1.00 ± 0.01, 0.90 ± 0.015, 0.79 ± 0.03, and 0.45 ± 0.05 Mev, together with gamma-rays at 82.6 ± 0.7, 200 ± 10, 440 ± 20 kev. The preponderant weight of the evidence appears to be against the assignment of so many beta- and gamma-rays.

The decay scheme given for this element in Fig. 28 is that due to Fraser. However, in view of the still somewhat conflicting evidence, the scheme may be open to revision.

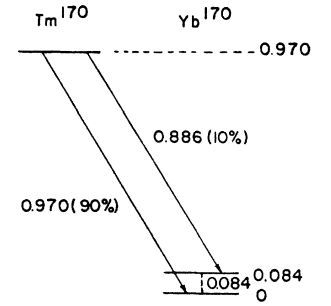

FIG. 28. Energy level diagram of Yb^{170}.

Ta^{181}

$Hf^{181} \xrightarrow{\beta} Ta^{181}$ Period 47 d.

The disintegration scheme of Hf^{181} is still open to some question. The original work of Hedgran, Hole, and Benes (H9, B13) gives one beta-ray group at 0.460 Mev together with three gamma-rays at 0.128, 0.342, and 0.472 Mev. DeBenedetti and McGowan (D12) have shown that there is a metastable state present of about 22-μsec. half-life. Recently, Chu and Wiedenbeck (C3) have reinvestigated the spectrum of Hf^{181} and find gamma-rays at 0.130, 0.134, 0.337, and 0.471 Mev, all of which are internally converted. They find one beta-ray group of energy 0.405 Mev. The results on the gamma-rays are essentially in agreement with the earlier work (H9) except for the occurrence of the line at 0.134 Mev. From the appearance of their curves this line seems to be real and, in addition, from energy considerations, it fits well into the decay scheme given in Fig. 29.

The line at 0.130 Mev is highly internally converted and the ratio N_K/N_L (not calculated by the authors) is estimated to be about 0.73. Using delayed coincidence techniques, DeBenedetti and McGowan (D12) and Lundby (L5, B12) have shown that the delay occurs between the emission of the 0.405-Mev beta-ray and

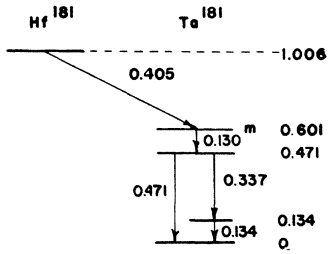

FIG. 29. Energy level diagram of Ta^{181}.

any gamma-rays, so that the metastable level, certainly connected with the emission of the 0.130-Mev converted gamma-ray, lies at the top of the level scheme of Ta^{181}. Standard-type coincidence experiments (M16, C3) have contributed nothing new to the solution of this problem. The scheme of Chu and Wiedenbeck is given in Fig. 29 for reference.

Mass $Hf^{181}=Ta^{181}+0.00108$.

Re^{187}

$W^{187} \xrightarrow{\beta} Re^{187}$ Period 24.1 hr.

Beach, Peacock, and Wilkinson (B10) have made a revision of the earlier work of Peacock and Wilkinson (P2) on W^{187}. There are two beta-ray groups at 0.63 (70 percent) and 1.33 (30 percent) Mev together with five gamma-rays at 0.078, 0.138, 0.480, 0.618, and 0.696 Mev. The rather complicated but well-substantiated scheme is given in Fig. 30.

Mass $W^{187}=Re^{187}+0.00143$.

Os^{186}

$Re^{186} \xrightarrow{\beta} Os^{186}$ Period 90 hr.

Measurements in the spectrograph have been made by Beach, Peacock, and Wilkinson (B9) who find one beta-ray at 1.073 ± 0.005 Mev and two gamma-rays in cascade of energies 0.138 ± 0.002 and 0.212 ± 0.002 Mev. The lower energy gamma-ray is internally converted. The disintegration scheme is shown in Fig. 31.

Mass $Re^{186}=Os^{186}+0.00153$.

Pt^{194}

$Au^{194} \xrightarrow{K} Pt^{194}$ Period 39 hr.

This transition has been investigated by Steffen, Huber, and Humbel (S19), partly by spectroscopic

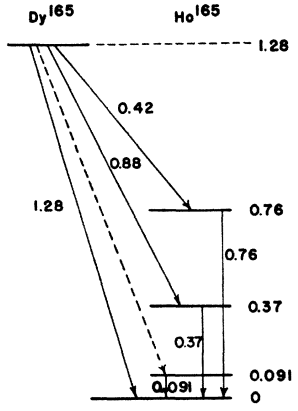

FIG. 27. Energy level diagram of Ho^{165}.

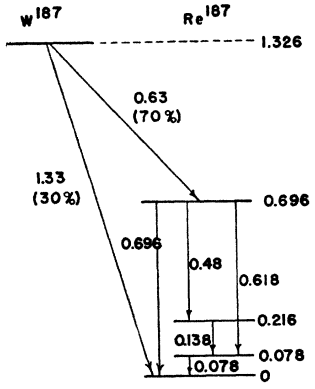

FIG. 30. Energy level diagram of Re^{187}.

means and partly by various types of coincidence counting. In addition to some low energy Auger lines, internal conversion lines at 0.291, 0.328, 0.466 Mev have been measured in a spectrograph. Since K, L, and M lines are found, the errors are probably not greater than 0.001 Mev.

Coincidence absorption of Compton electrons shows two additional gamma-rays at 2.1 and 1.48 Mev. The intensity ratio of these two gamma-rays is $I_{1.48}/I_{2.1}=2.3$. Gamma-gamma-absorption experiments suggest that the lines at 1.48, 0.328, and 0.291 are in cascade and that the three are in parallel with the one at 2.1. This seems likely from energy considerations. The line at 0.466 Mev, which seems to have no other place in the scheme, is placed above the 2.1-Mev level, as is shown in Fig. 32.

In view of the fact that the energy of the high energy gamma-rays was not measured by spectroscopic means and also since the authors do not appear to have performed any chemical separation on their source, the disintegration scheme cannot be considered to be as certain as the others in this survey.

Pt^{195}

$Au^{195} \xrightarrow{K} Pt^{195}$ Period 180 d.

Steffen, Huber, and Humbel (S19) find conversion lines for two gamma-rays at 0.129 and 0.096 Mev. They find x-gamma- and x-beta-coincidences but no beta-beta-coincidences, from which they conclude that the two gamma-rays are not in cascade. Their disintegration scheme is shown in Fig. 32.

Hg^{198}

$Au^{198} \xrightarrow{\beta} Hg^{198}$ Period 2.8 d.

This disintegration has been the subject of a large amount of investigation by spectrographic, absorption, and coincidence techniques. Earlier work (L6) in which several gamma-rays and two beta-ray groups were found, has not been substantiated and is thought to be due to impurities. The spectrographic work of Peacock and Wilkinson (P2), Siegbahn and Hedgran (S20) as well as the coincidence work of Jurney (J2) are all in agreement. The beta-ray spectrum is simple with an end point of 0.97±0.01 Mev (P2) followed by an internally converted gamma-ray of energy 0.4110 ±0.001 Mev (S20). DuMond, Lind, and Watson (D13) have measured the energy of the gamma-ray with a crystal spectrometer and find the value 0.41118±0.00005 Mev. The latest values for the internal conversion coefficients (S20) are $\alpha_K=3.0$ percent, $\alpha_L=1.0$ percent, and $\alpha_M\sim 0.3$ percent. The disintegration scheme is given in Fig. 33.

Mass $Au^{198}=Hg^{198}+0.00148$.

Hg^{199}

$Au^{199} \xrightarrow{\beta} Hg^{199}$ Period 3.3 d.

Spectrographic work of Beach, Peacock, and Wilkinson (B8) and coincidence studies (M17, M14) indicate that the beta-ray spectrum is simple and followed by several gamma-rays. The beta-ray energy is 0.32 Mev. There are five gamma-rays at 0.024, 0.051, 0.070, 0.156, 0.207, and 0.230 Mev. The disintegration scheme is given in Fig. 33.

Mass $Au^{199}=Hg^{199}+0.00059$.

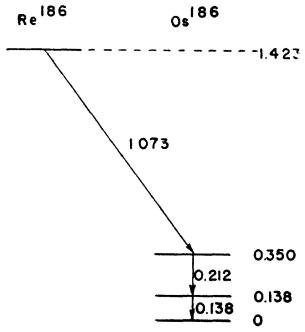

FIG. 31. Energy level diagram of Os^{186}.

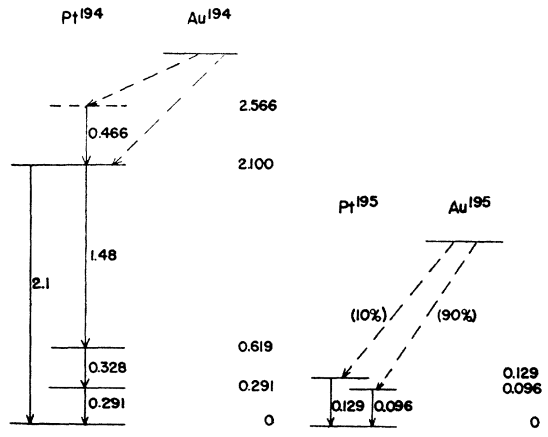

FIG. 32. Energy level diagram of Pt^{194} and Pt^{196}.

Tl^{203}

$Hg^{203} \xrightarrow{\beta} Tl^{203}$ Period 43.5 d.

Saxon (S21) and Slätis and Siegbahn (S22) have made a spectroscopic investigation of this element and obtain results substantially in agreement. There is one beta-ray of energy 0.208±0.003 Mev followed by a single gamma-ray of energy 0.279±0.002. The value of the conversion ratio is $N_K/N_L=3$. Slätis and Siegbahn (S22) used an isotopically separated source of Hg^{203} for their experiments. The disintegration scheme is given in Fig. 34.

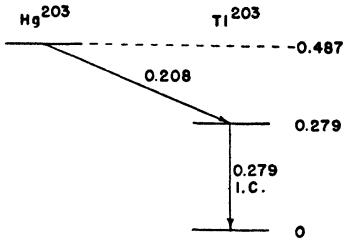

FIG. 34. Energy level diagram of Tl^{203}.

Mass $Hg^{203}=Tl^{203}+0.00523=203.055$.

IV. GENERAL DISCUSSION

The sixty disintegration schemes discussed in the previous section are distributed widely over the periodic table and give a good cross section of the types of spectra encountered and the general trend of nuclear energy levels. Information concerning many of the rare earths is lacking, owing to the difficulty of chemical procedures in this region of the periodic table. The writer believes that the disintegration schemes described in this report are sufficiently self-consistent that further work will only make minor modifications in them. There is a considerable possibility that more low energy lines—below 0.150 Mev—may be discovered in these schemes, since some of them were determined before the advent of thin window techniques.

In looking around for regularities in nuclear spectra, one considers first what happens to the levels in a series of isotopes in which the number of neutrons is increased. Eleven such series are presented in this report and are shown in Fig. 7 (Ti), Fig. 8 (Cr), Fig. 9 (Fe), Fig. 16 (Sr), Fig. 17 (Mo), Fig. 21 (In), Fig. 22 (Te), Fig. 23 (Xe), Fig. 24 (Ba), Fig. 32 (Pt), Fig. 33 (Hg). It will be seen, in looking at these figures, that the addition of *two neutrons* makes very little difference in the position of the lowest level, whereas the addition of an odd neutron usually produces many more low lying levels. This is most striking in the series for Xe and that for Te. It should be remembered that in the Xe series, the lower levels of Xe^{130} are in cascade and hence their position is arbitrary. It is quite possible that the lowest level of Xe^{130} is 0.537 Mev rather than 0.744 Mev. There are three striking exceptions to this rule, namely, Cr, Fe, and Ba. In the case of the Ba isotopes the parent of Ba^{137}, Cs^{137}, is a "magic number" nucleus. The beta-ray spectrum of Cs^{137} has a forbidden shape and Ba^{137} has a metastable state. These two facts and the fact that Ba^{137} has as wide a spacing as Ba^{134} are no doubt connected with the "magic numbers." There seems to be no such explanation for the fact that Fe^{55} has as wide a spacing as Fe^{56} and Fe^{58}. The pair Cr^{52}, Cr^{54} is not in agreement with this rule.

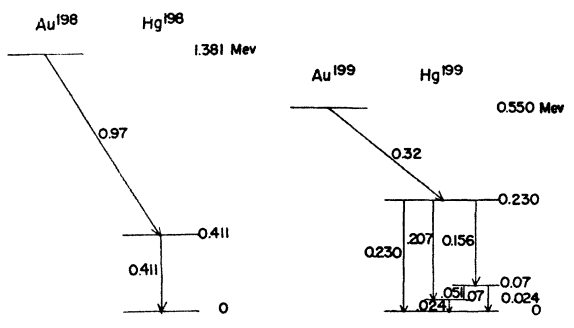

FIG. 33. Energy level diagram of Hg^{198} and Hg^{199}.

Finally, the spacing of the levels, in any given nucleus, is larger than would be expected from the liquid drop model or other statistical models of the nucleus. This may be due to the action of selection rules or other causes not yet well understood. The spacing of the levels does, however, become smaller as the number of particles in the nucleus increases. There is also a tendency for nuclei consisting of an odd number of particles to have more low lying levels than those containing an even number. This tendency is more marked from the middle of the periodic table onward.

This work was assisted by the joint program of the ONR and AEC. The author wishes to express his thanks to Dr. C. L. Peacock, Dr. F. C. Maienschein, and Mr. W. S. Cuffey for their help in preparing the figures.

BIBLIOGRAPHY

A1. D. E. Alburger, Phys. Rev. **76**, 435 (1949).
A2. H. M. Agnew, thesis (Chicago).
B1. E. L. Brady and M. Deutsch, Phys. Rev. **72**, 870 (1947).
B2. E. L. Brady and M. Deutsch, Phys. Rev. **74**, 1541 (1948).
B3. Benes, Hedgran, and Hole, Arkiv. f. Mat. Astr. o. Fys. **35A**, No. 12 (1947).
B4. E. Bleuler and W. Zünti, Helv. Phys. Acta **20**, 196 (1947).
B5. Bradt, Gugelot, Huber, Medicus, Preiswerk, and Scherrer, Helv. Phys. Acta **18**, 259 (1945).
B6. R. Bouchez and G. A. Renard, J. de phys. et rad. **8**, 289 (1947).
B7. Brosi, DeWitt, and Zeldes, Phys. Rev. **75**, 1615 (1949).
B8. Beach, Peacock, and Wilkinson, Phys. Rev. **76**, 1624 (1949).
B9. Beach, Peacock, and Wilkinson, Phys. Rev. **75**, 1585 (1949).
B10. Beach, Peacock, and Wilkinson, Phys. Rev. **75**, 211 (1949).
B11. S. W. Barnes, Phys. Rev. **56**, 414 (1939).
B12. Bunyan, Lundby, Ward, and Walker, Proc. Phys. Soc. **61**, 300 (1948).
B13. Benes, Ghosh, Hedgran, and Hole, Nature **162**, 261 (1948).
C1. B. R. Curtis and J. R. Richardson, Phys. Rev. **57**, 1121 (1940).
C2. C. S. Cook and L. M. Langer, Phys. Rev. **73**, 1149 (1948).
C3. K. Y. Chu and M. Y. Wiedenbeck, Phys. Rev. **75**, 226 (1949).

D1. DuMond, Lind, and Watson, Phys. Rev. **74**, 1561(A) (1947).
D2. DuMond, Lind, and Watson, Phys. Rev. **75**, 1226 (1948).
D3. M. Deutsch and L. G. Elliott, Phys. Rev. **65**, 211 (1944).
D4. M. Deutsch and A. Hedgran, Phys. Rev. **75**, 1443 (1949).
D5. Deutsch, Elliott, and Roberts, Phys. Rev. **68**, 193 (1945).
D6. Downing, Deutsch, and Roberts, Phys. Rev. **60**, 470 (1941).
D7. Deutsch, Roberts, and Elliott, Phys. Rev. **61**, 389A (1942).
D8. M. Deutsch, Phys. Rev. **72**, 527(A) (1947).
D9. M. Dode and B. Pontocorvo, Comptes Rendus **207**, 287 (1938).
D10. S. D. Drell, Phys. Rev. **75**, 132 (1949).
D11. Downing, Deutsch, and Roberts, Phys. Rev. **61**, 686 (1947).
D12. S. DeBenedetti and F. K. McGowan, Phys. Rev. **70**, 569 (1946).
D13. DuMond, Lind, and Watson, Phys. Rev. **73**, 1392 (1948).
D14. Deutsch, Downing, Elliott, Irvine, and Roberts, Phys. Rev. **62**, 3 (1942).

E1. L. G. Elliott and R. E. Bell, Phys. Rev. **74**, 1869 (1948).
E2. L. G. Elliott and M. Deutsch, Phys. Rev. **64**, 321 (1943).
E3. T. Enns, Phys. Rev. **56**, 872 (1939).
E4. W. S. Emmerich and J. D. Kurbatov, Phys. Rev. **75**, 1446 (1949).
E5. L. G. Elliott and R. E. Bell, Phys. Rev. **72**, 979 (1947).

F1. I. Feister and L. F. Curtis, J. Research Nat. Bur. of Stand. **38**, 411 (1947).
F2. Friedlander, Goldhaber, and Scharff-Goldhaber, Phys. Rev. **74**, 981 (1948).
F3. J. S. Fraser, Phys. Rev. **76**, 1540 (1949).

G1. L. H. Gray, Proc. Camb. Phil. Soc. **27**, 103 (1931).
G2. Good, Peaslee, and Deutsch, Phys. Rev. **69**, 313 (1946).
G3. R. L. Graham and G. H. Tomlin, Nature **164**, 278 (1949).
G4. P. J. Grant and R. Richmond, Nature **163**, 840 (1949).

H1. W. F. Hornyak and T. Lauritsen, Rev. Mod. Phys. **20**, 191 (1948).
H2. D. R. Hamilton, Phys. Rev. **58**, 122 (1940).
H3. Hornyak, Lauritsen, and Rasmussen (unpublished), see L1.
H4. N. Hole and K. Siegbahn, Arkiv. f. Mat. Astr. o. Fys. **33A**, No. 9 (1947).
H5. S. K. Haynes, Phys. Rev. **73**, 187 (1948).
H6. Huber, Medicus, Preiswerk, and Steffen, Phys. Rev. **73**, 1211 (1948).
H7. J. E. Hudgens, Jr. and W. S. Lyon, Phys. Rev. **75**, 206 (1949).
H8. N. Hole, Arkiv. f. Mat. Astr. o. Fys. **34B**, No. 19 (1947).
H9. Hedgran, Hole, and Benes, Arkiv. f. Mat. Astr. o. Fys. **35A**, No. 33 (1948).
H10. Hill, Scharff-Goldhaber, and Friedlander, Phys. Rev. **75**, 324 (1949).

I1. Z. Itoh, Proc. Phys. Math. Soc. Japan **23**, 405 (1941).

J1. Jensen, Laslett, and Pratt, Phys. Rev. **75**, 458 (1949).
J2. E. T. Jurney, Phys. Rev. **74**, 1049 (1948).
J3. E. T. Jurney, Phys. Rev. **76**, 290 (1949).
J4. E. T. Jurney and A. C. G. Mitchell, Phys. Rev. **73**, 1153 (1948).
J5. Jensen, Laslett, and Pratt, Phys. Rev. **76**, 430 (1949).

K1. E. J. Konopinski, Rev. Mod. Phys. **15**, 209 (1943).
K2. F. N. D. Kurie and M. Ter-Pogossian, Phys. Rev. **74**, 677 (1948).
K3. Kern, Mitchell, and Zaffarano, Phys. Rev. **76**, 94 (1949).
K4. Kern, Mitchell, and Zaffarano, Phys. Rev. **73**, 1142 (1948).
K5. B. H. Kettelle, Oak Ridge Quarterly (May, 1949).

L1. T. Lauritsen, Nat. Research Council, Nuclear Science Series, Report No. 5.
L2. L. M. Langer and H. C. Price, Phys. Rev. **75**, 1109 (1949).
L3. J. L. Lawson and J. M. Cork, Phys. Rev. **57**, 982 (1940).
L4. Lind, Brown, Klein, Müller, and DuMond, Phys. Rev. **75**, 1544 (1949).
L5. A. Lundby, thesis, Birmingham (1948).
L6. P. Levy and E. Greuling, Phys. Rev. **73**, 83 (1948).
L7. Lind, Brown, and DuMond, Phys. Rev. **76**, 591 (1949).

M1. A. C. G. Mitchell, Rev. Mod. Phys. **20**, 296 (1948).
M2. L. Meitner, Arkiv. f. Mat. Astr. o. Fys. **32A**, No. 6 (1945).
M3. A. E. Miller and M. Deutsch, Phys. Rev. **72**, 527 (1947).
M4. L. C. Miller and L. F. Curtiss, Phys. Rev. **70**, 983 (1946).
M5. J. Martelly, Comptes Rendus **216**, 838 (1944).
M6. F. C. Maienschein and J. L. Meem, Jr., Phys. Rev. **76**, 899 (1949).
M7. Mitchell, Zaffarano, and Kern, Phys. Rev. **73**, 1424 (1948).
M8. L. C. Miller and L. F. Curtiss, Phys. Rev. **70**, 983 (1946).
M9. Mitchell, Langer, and McDaniel, Phys. Rev. **57**, 1107 (1940).
M10. W. E. Meyerhoff and G. Scharff-Goldhaber, Phys. Rev. **72**, 273 (1947).
M11. Mitchell, Mei, Maienschein, and Peacock, Phys. Rev. **76**, 1450 (1949).
M12. F. Metzger and M. Deutsch, Phys. Rev. **74**, 1640 (1948).
M13. Moe, Owen, and Cook, Phys. Rev. **75**, 1270 (1949).
M14. J. L. Meem, Jr. and F. C. Maienschein, Phys. Rev. **76**, 328 (1949).
M15. A. C. G. Mitchell and C. L. Peacock, Phys. Rev. **75**, 197 (1949).
M16. Mandeville, Scherb, and Keighton, Phys. Rev. **75**, 221 (1949).
M17. Mandeville, Scherb, and Keighton, Phys. Rev. **74**, 601 (1948).
M18. Medicus, Mukerji, Preiswerk, and de Saussure, Phys. Rev. **74**, 839 (1948).

O1. F. Oppenheimer and E. P. Tomlinson, Phys. Rev. **56**, 858(A) (1939).
O2. R. K. Osborne and M. Deutsch, Phys. Rev. **71**, 467(A) (1947).
O3. Owen, Moe, and Cook, Phys. Rev. **74**, 1879 (1948).
O4. R. K. Osborne and W. C. Peacock, Phys. Rev. **69**, 679 (1946).

P1. C. L. Peacock and A. C. G. Mitchell, Phys. Rev. **75**, 1272 (1949).
P2. C. L. Peacock and R. G. Wilkinson, Phys. Rev. **74**, 297 (1948).
P3. W. C. Peacock and M. Deutsch, Phys. Rev. **69**, 306 (1945).
P4. E. C. Pollard, Phys. Rev. **54**, 411 (1938).
P5. W. C. Peacock, see S1.
P6. W. C. Peacock and J. W. Jones, Plutonium Project Reports, CNL-14 (February, 1948) as reported in S1.
P7. W. C. Peacock, Phys. Rev. **72**, 1049 (1947).
P8. Peacock, Jones, and Overman, Plutonium Project Report as reported in S1.

R1. Ramsey, Meem, and Mitchell, Phys. Rev. **72**, 639 (1947).
R2. Rose, Goertzel, Spinrad, Harr, and Strong, *Tables of K-Shell Internal Conversion Coefficients* (privately distributed prior to publication).
R3. G. A. Renard, Comptes Rendus **223**, 945 (1946).
R4. W. Rall and R. G. Wilkinson, Phys. Rev. **71**, 321 (1947).
R5. Roberts, Elliott, Downing, Peacock, and Deutsch, Phys. Rev. **64**, 268 (1943).
R6. Roberts, Downing, and Deutsch, Phys. Rev. **60**, 544 (1941).
R7. Robinson, Ter-Pogossian, and Cook, Phys. Rev. **75**, 1099 (1949).

S1. G. T. Seaborg and I. Perlman, Rev. Mod. Phys. **20**, 585 (1948).
S2. E. Segrè and A. C. Helmholz, Rev. Mod. Phys. **21**, 271 (1949).
S3. F. B. Shull and E. Feenberg, Phys. Rev. **75**, 1768 (1949).
S4. K. Siegbahn, Phys. Rev. **70**, 127 (1947).
S5. K. Siegbahn, Proc. Roy. Soc. **A188**, 541 (1947).
S6. K. Siegbahn, Arkiv. f. Mat. Astr. o. Fys. **34**, No. 4 (1946).
S7. K. Siegbahn and A. Johanson, Arkiv. f. Mat. Astr. o. Fys. **34**, No. 10 (1946).
S8. G. P. Smith, Phys. Rev. **61**, 578 (1942).
S9. K. Siegbahn, Arkiv. f. Mat. Astr. o. Fys. **33A**, No. 10 (1946).
S10. K. Siegbahn (private communication).
S11. K. Siegbahn, Arkiv. f. Mat. Astr. o. Fys. **34**, No. 7 (1946).
S12. K. Siegbahn, Phys. Rev. **75**, 1277 (1949) (also private communication).
S13. K. Siegbahn (private communication).
S14. K. Siegbahn and N. Hole, Phys. Rev. **70**, 133 (1946).
S15. K. Siegbahn and M. Deutsch, Phys. Rev. **71**, 483 (1947).
S16. K. Siegbahn and M. Deutsch, Phys. Rev. **73**, 410 (1948).
S17. H. Slätis, Arkiv. f. Mat. Astr. o. Fys. **33A**, No. 17 (1946).
S18. D. Saxon and L. Richards, Phys. Rev. **76**, 186 (1949).
S19. Steffen, Huber, and Humbel, Helv. Phys. Acata **22**, 167 (1949).
S20. K. Siegbahn and A. Hedgran, Phys. Rev. **75**, 523 (1949).
S21. D. Saxon, Phys. Rev. **74**, 849 (1948).
S22. H. Slätis and K. Siegbahn, Phys. Rev. **75**, 318 (1949).
S23. K. Siegbahn and A. Ghosh, Phys. Rev. **76**, 307 (1949).

T1. C. M. Turner, Phys. Rev. **76**, 148 (1949).
T2. Townsend, Owen, Cleland, and Hughes, Phys. Rev. **74**, 99 (1948).
T3. Townsend, Cleland, and Hughes, Phys. Rev. **74**, 499 (1948).

W1. M. L. Wiedenbeck, Phys. Rev. **66**, 36 (1944).
W2. M. L. Wiedenbeck, Phys. Rev. **67**, 59 (1945).
W3. M. L. Wiedenbeck and K. Y. Chu, Phys. Rev. **72**, 1164 (1947).

Z1. Zaffarano, Kern, and Mitchell, Phys. Rev. **74**, 105 (1948).
Z2. Zaffarano, Kern, and Mitchell, Phys. Rev. **74**, 682 (1948).